Elastin-like recombinamers as substrates for retinal pigment epithelial cell growth

Girish K. Srivastava,[1,2] Laura Martín,[3] Amar K. Singh,[1] Ivan Fernandez-Bueno,[1] Manuel J. Gayoso,[1] Maria T. Garcia-Gutierrez,[1] Alessandra Girotti,[3] Matilde Alonso,[3] José C. Rodríguez-Cabello,[3] José C. Pastor[1]

[1]Institute of Applied Ophthalmobiology (IOBA), University of Valladolid, Valladolid, Spain
[2]Castilla and Leon Regenerative Medicine and Cell Therapy Network Center, Spain
[3]G.I.R. BIOFORGE Group, University of Valladolid, CIBER-BBN, Valladolid, Spain

Received 3 August 2010; revised 17 December 2010; accepted 10 January 2011
Published online 25 March 2011 in Wiley Online Library (wileyonlinelibrary.com). DOI: 10.1002/jbm.a.33050

Abstract: The aim of this study is to investigate the use of elastin-like recombinamers (ELRs) as a substrate that can maintain the growth, phenotype, and functional characteristics of retinal pigment epithelial (RPE) cells efficiently and as a suitable carrier for the transplantation of autologous RPE cells for treatment of age-related macular degeneration (AMD). ELR films containing a bioactive sequence, RGD (ELR-RGD), and one with no specific sequence (ELR-IK) as control, were obtained by solvent-casting onto glass and subsequent cross-linking. ARPE19 cells were seeded on sterilized ELR films as well as on the control surfaces. Cells were analysed after 4, 24, 72, and 120 h to study cell adhesion, proliferation, cell viability, morphology, and specificity by staining with Trypan blue, DAPI, Rhodamin-Phalloidin and RPE65, ZO-1 antibodies and observing under fluorescence as well as electron microscope. ARPE19 cells seeded on both ELR films and controls were 100% viable and maintained their morphology and set of characteristics at the different time points studied. Cell proliferation on ELR-RGD was significantly higher than that found on ELR-IK at all time points, although it was less than the growth rate on polystyrene. ARPE19 cells grow well on ELR-RGD maintaining their phenotype. These results should be extended to further studies with fresh human RPE cells and *in vivo* studies to determine whether this ELR-RGD matrix could be used as a Bruch's membrane prosthesis and carrier for transplantation of RPE cells in patients suffering with AMD. J Biomed Mater Res Part A: 97A: 243–250, 2011.

Key Words: regenerative medicine, biomaterial, RPE cells, AMD, elastin-like recombinamers

INTRODUCTION

Age-related macular degeneration (AMD) is the leading cause of irreversible severe vision loss and legal blindness in patients over 65 years. Furthermore, the prevalence of this disease (8%) increases steeply with age.[1,2]

There are basically two clinical forms of AMD: wet (or neovascular) and dry (or atrophic). Wet AMD can currently be treated with anti-vascular endothelial growth factors (anti-VEGF), whereas dry AMD, which accounts for the majority of cases (60–80%), cannot as yet be treated, even palliatively.[3] Despite intense basic and clinical research efforts, the pathology of AMD is not completely understood, although it appears to be a multifactorial disease involving a complex interaction between metabolic, functional, genetic, and environmental factors.[4] It is well known that disease-related alterations, at least in the initial stages of AMD, are limited to the external layers of the retina, which in theory can be repaired using cell therapy approaches.[5–8] Retinal pigment epithelium (RPE) plays a pivotal role in normal retinal functioning, including the transport of nutrients from the choroidal blood vessel layer to the photoreceptors, elimination of their waste and formation of the blood-retina barrier that controls the transport of substances into the retina.[9] The accumulation of drusen, basal deposits and advanced glycation end products (AGEs) below the RPE layer as a result of dysfunction of the diseased RPE are typical signs of AMD that probably contribute to damage of the Bruch's membrane (BrM), which supports the RPE cells and maintains their health, polarity and functionality, and photoreceptors.[10] Over the last 25 years, several approaches, such as patch graft transplant, RPE transplantation and macular translocation, have shown that replacing diseased RPE with healthier autologous RPE in selected cases can rescue photoreceptors, prevent further visual loss, or even promote visual improvement in both humans and animals.[11–16]

It is also known that *ex vivo* expansion of adult RPE cells offers the potential to partially reverse the influence of aging, although there is a high risk of cell transdifferentiation.[17–21] The best results are obtained when these adult

Correspondence to: G. K. Srivastava; e-mail: girish@ioba.med.uva.es
Contract grant sponsors: Castilla and Leon Regenerative Medicine and Cell Therapy Network Center, CIBER-BBN, AECI (Part of the Spanish Ministry of Foreign Affairs), The Junta de Castilla-León
Contract grant sponsor: National Plan of I+D+I 2008-2011 and Spanish Institute of Health Carlos III (ISCIII)-Subdireccion General de Evaluacion y Fomento de la Investigacion (MICNN) with confinantiation FEDER; contract grant number: PS09/00938

autologous RPE cells are in contact with an appropriate extracellular matrix (ECM) that provides appropriate physiological signals to maintain their differentiated state, polarity, phenotype, and functional characteristics.[22] Numerous biocompatible natural or synthetic ECMs have been investigated as transplant vehicles in the last few years, although the latest studies in this field have shown that unfavorable characteristics of these ECMs lead to neural retinal atrophy.[10] The development of an appropriate biocompatible substrate is therefore vital. This substrate must be in the form of a flexible thin film so that it can be handled easily during surgical transplantation. It must also be able to support and maintain an organized monolayer of healthy RPE cells and must have bioactive domains that provide physiological signals to cells to ensure they maintain all their characteristics *in vivo* after transplantation, a porous structure to allow exchange of materials in and out of the RPE monolayer, thereby supporting the survival of other cell layers in the retina, including, photoreceptors, and must not form toxic by-products upon biodegradation. The elastin-like recombinamers (ELRs) developed by a group at our university could be useful in this respect[23,24] as other ELRs provided by the same group have been shown to be suitable for tissue engineering to restore vision by reconstructing the ocular surface.[25]

Genetic engineering techniques involving protein-based polymers have allowed the design and synthesis of new advanced materials with an unrivalled degree of complexity and control that can incorporate structural and functional domains derived from ECM proteins almost at will. These recombinant polymers offer the possibility to obtain materials that combine some of the complex properties found in natural proteins with functions of particular interest that are not displayed in the living organism. ELRs have been attracting interest because of their excellent biocompatibility, mechanical properties and bioactivity, amongst others.[26–28]

In this study, we investigated the suitability of an ELR film containing bioactive RGD sequence for allowing the growth of a monolayer of RPE with maintaining their characteristics for future subretinal transplantation.

MATERIALS AND METHODS

ELR expression and purification

Standard molecular biology techniques were used to construct two ELR genes containing a bioactive domain (ELR-RGD and ELR-IK). ELR-RGD contains a peptide loop present in the human fibronectin protein with the well-known arginine-glycine-aspartic acid (RGD) sequence for cell adhesion.[29,30] ELR-IK, which has no bioactive domain, was used as negative control.

Polymer production was carried out using cellular systems for genetically engineered protein biosynthesis in *Escherichia coli*. Synthetic oligonucleotides were purchased from IBA GmbH (Goettingen, Germany), and *Taq* DNA polymerase and the restriction enzyme Eam 1104 I were purchased from Stratagene (La Jolla, CA). The restriction enzymes *Xba*I, *Hind*III, *Dpn*I, *Eco*RI, and *Sap*I were purchased from Fermentas (Burlington, ON), and T4 DNA ligase, Shrim Alkaline Phosphatase (S.A.P), and Antartic alkaline phosphatase were purchased from New England Biolabs (Beverly, Ma). PCR amplifications were performed in an Eppendorf AG 22331 thermocycler. Gel photographs were taken with the Gel logic 100 Imaging System running the Kodak 3.6 software. *Escherichia coli* BLR (DE3) strain and the expression vector pET (25+) from Novagen (Madison WI), and Ampicillin from Apollo Scientific (Bredbury, UK), were used during elastin-like recombinamer (ELR) production, which was performed with several cycles of temperature-dependent reversible precipitation, as described elsewhere.[24]

The purity and molecular weight of the proteins were verified by SDS-PAGE gels and mass spectrometry (MALDI-TOF/MS), whereas the correctness of the sequence was checked by amino acid analysis and amino acid sequencing. Physical properties were characterized by differential scanning calorimetry (DSC) and turbidity measurements.

The amino-acid sequences of the ELRs used in this work are depicted below:

ELR-RGD: MGSS-H_6-SSGLVPRGSHMESLLP-{[$(VPGIG)_2$(VPGKG)$(VPGIG)_2]_2$AVTG**RGD**SPASS[$(VPGIG)_2$(VPGKG)$(VPGIG)_2]_2\}_6$
(M_w = 60,661 Da).

ELR-IK: MESLLP-$(VPGIG\text{-}VPGIG\text{-}VPGKG\text{-}VPGIG\text{-}VPGIG)_{24}$-V
(M_w = 51,980 Da).

Preparation of ELR films

ELR-films were obtained by solvent-casting onto glass and subsequent cross-linking with hexamethylene diisocyanate (HDI), a lysine-targeted homobifunctional crosslinker, as described elsewhere.[31]

Thus, an aqueous ELR solution (80 μL, 50 mg/mL) was deposited on circular cover glasses (diameter: 12 mm; Thermo Scientific, Madrid Spain). After incubation for 8 h at 60°C, the dry films were cross-linked by immersion in 10% HDI/acetone solution overnight and then exhaustively washed with type I water. All reagents were purchased from Sigma Aldrich, Madrid Spain.

The ELR films and controls (glass, polystyrene) were placed in a 24-well cell-culture plate, sterilized for 12 h under UV light, and then incubated in Dulbecco's Modified Eagle Medium (DMEM; Invitrogen, Paisley, UK) with antibiotics for 2 h before cell seeding.

Cell culture

ARPE19 cells were used for all quantitative and qualitative analysis in this study. These cells[32] were obtained from the American Type Culture Collection ATCC (Manassas, VA) and maintained in a 1:1 (v/v) mixture of DMEM/F12 supplemented with 10% FBS, 2 m*M* L-glutamine, 50 U/mL penicillin G, 50 mg/mL streptomycin, and 2.5 mg/mL amphotericin B (Invitrogen-Gibco, Paisley, UK). Cells were maintained in a humidified atmosphere at 37°C in the presence of 5% CO_2, and the medium was replaced every 3 days until confluence was reached. Cells were then detached with 0.1% trypsin and 0.04% tetrasodium ethylenediaminetetraacetate (EDTA)

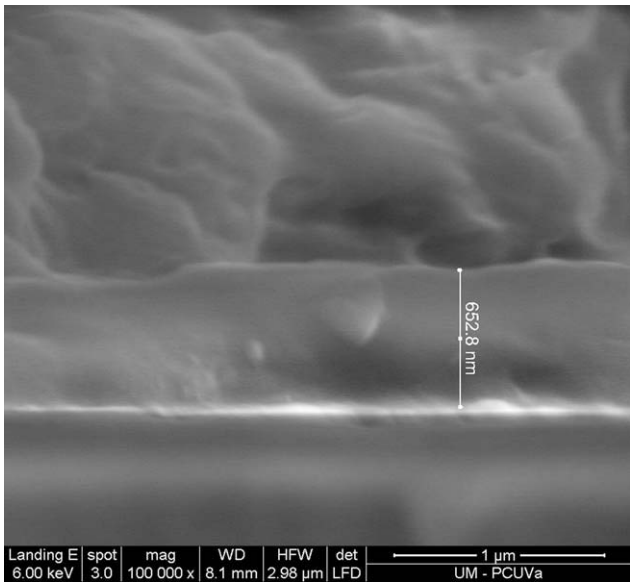

FIGURE 1. SEM of ELR-RGD film showed 652.8 nm thickness of the polymeric film.

(Invitrogen-Gibco, Paisley, UK), mixed with complete medium to block the trypsin-EDTA activity, and washed and resuspended in phosphate-buffered saline (PBS; Invitrogen-Gibco, Paisley, UK).

Cell numbers and viability were determined by standard Trypan blue exclusion assay. 1×10^4 ARPE19 cells were seeded on ELR-RGD film scaffold and controls (ELR-IK, the polystyrene substrate of standard tissue culture plates and glass) and incubated under standard conditions for up to 120 h.

Cell number quantification

At defined time periods after cell seeding, the substrates were washed with PBS to remove nonadhered cells and the cell numbers were determined by manual counting using a phase contrast and fluorescence microscope (Leica Microsystems, Mannheim, Germany). Cells were nuclear stained with DAPI (Invitrogen, Eugene, OR) for 1 min at room temperature (RT), mounted in a fluorescent mounting medium (Invitrogen, Paisley, UK), and visualized using a fluorescence microscope. Twenty fields (×10) were photographed at random per substrate. The cells, and their nuclei, contained in each field were counted using Adobe Photoshop Elements software. The mean number of nuclei per field of view (×10) was calculated for each time interval for each treatment and presented as a histogram showing the average nuclear count per field of view ±1 standard deviation (SD) versus time.

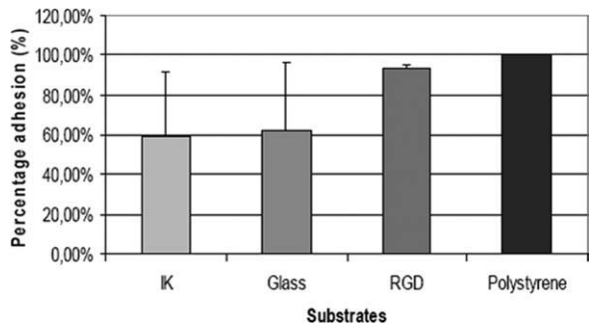

FIGURE 2. Percentage of ARPE19 cells adhered to different substrates at 4 h. The data presented are the mean number of cells (phase-contrast microscopy as well as nuclear counts of cells, assuming 1 nucleus per cell) per field (×10) attached to each surface at 4 h as a percentage of the control (polystyrene) ±1 SD. This histogram shows that the ELR-RGD surface supports adhesion of ARPE19 cells to lesser extent than polystyrene surface but is nevertheless higher than that for ELR-IK and glass. $p < 0.05$ is considered significant for comparing the percentage of adhered cells on different surfaces.

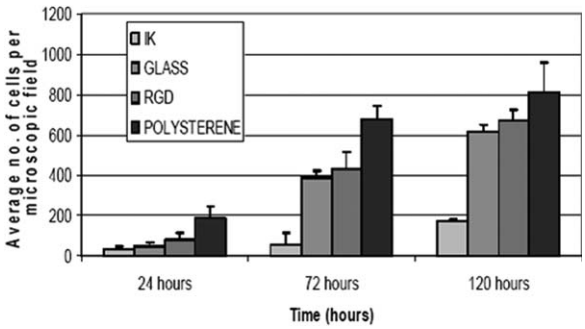

FIGURE 3. Growth of ARPE19 cells on each substrate studied. The histogram shows the mean number of cells (phase-contrast microscopy as well as nuclear counts of cells, assuming 1 nucleus per cell) on different substrates (ELR-RGD, ELR-IK, polystyrene, and glass) at different time intervals (24, 72, and 120 h). The data are presented as mean number of cells per field (×10) ±1 SD. The ELR-RGD, polystyrene, and glass substrates are more favorable for cell growth than ELR-IK. $p < 0.05$ is considered significant for comparing the number of cells growing on different surfaces.

Cytotoxicity

The cytotoxicity of all substrates was analyzed after 4, 24, 72, and 120 h incubation. Thus, the substrates were washed with PBS, the cells stained with Trypan blue and viewed immediately under an optical microscope. Twenty fields (×10) of each substrate were photographed at random and the mean number of nonstained cells per field of view (×10) was taken as the number of surviving cells. The total number of stained and nonstained cells at 4, 24, 72, and 120 h was calculated as detailed above.

Cell adhesion

Cells were counted after 4 h, under a phase-contrast microscope, to determine the cell attachment to ELR films and control surfaces, as detailed above. For cell adhesion determination, the average number of cells on the polystyrene substrate (positive control) was set to 100% and the average number of cells on the other substrates (ELR-RGD, ELR-IK, and Glass) calculated as a percentage of the cells growing on the polystyrene surface. For the quantification at 4 h, the values presented are the mean number of cells per field (×10) attached to each substrate as a percentage of the polystyrene control ±1 SD.

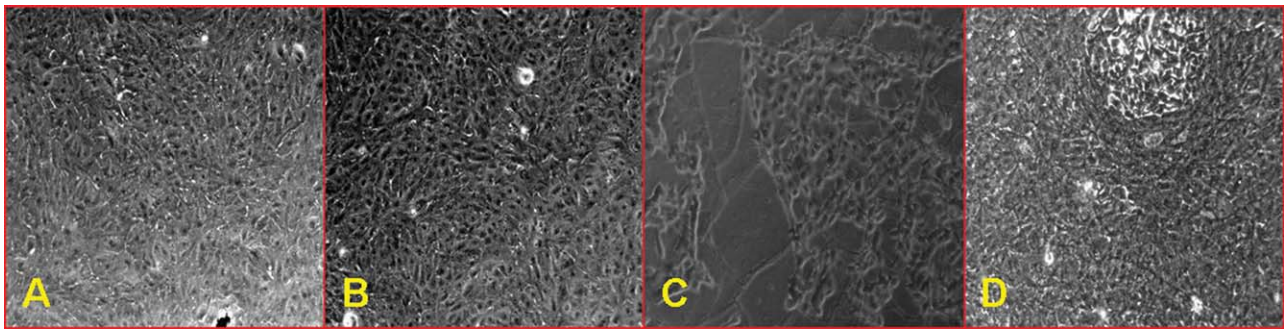

FIGURE 4. Growth of ARPE19 cells on different substrates. Phase-contrast microscopy demonstrates the cell density as well as the hexagonal morphology and the mosaic pattern of ARPE19 cells on each substrate studied at 120 h. ELP-IK does not support the growth of ARPE19 cells. (A) Polystyrene; (B) glass; (C) ELR-IK; (D) ELR-RGD. [Color figure can be viewed in the online issue, which is available at wileyonlinelibrary.com.]

Cellular morphology and specificity assessment

The epithelial morphology of the cells growing on each substrate was determined by staining cytoskeleton actin filaments with Rhodamine-Phalloidin (Molecular Probes-Invitrogen, Paisley, UK) and tight junction with anti-ZO-1 antibody (Invitrogen, Camarillo, CA), whereas cell specificity was studied by an immunostaining technique against the RPE65 antigen (Novus Biologicals, Inc., Littleton, CO), a specific marker of RPE.[32] At each time point the cells were washed with PBS (3 × 5 min), fixed with 4% paraformaldehyde for 10 min, permeabilized with PBT (0.2% TritonX-100 in PBS) for 10 min, washed with PBS (3 × 5 min) and blocked for 1 h in antibody blocking buffer (10% Normal goat serum, 1% Bovine serum albumin in PBT). The cells were then incubated with a 1:100 dilution of anti-RPE65 antibody or with a 1:50 dilution of anti-ZO-1 antibody in PBT overnight at 4°C, then washed with PBT (3 × 5 min) and incubated with a 1:100 dilution of anti-mouse IgG-FITC (Jackson Immunoresearch Laboratories, Inc., West Grove, PA) in PBS for 1 h at room temperature. The cells were also costained with a 1:40 dilution of Rhodamine-Phalloidin (200 unit/mL) in PBS for 20 min, then mounted and observed under a fluorescence microscope, as described above.

The presence of intercellular tight junction and gap junction between the cells grown on each substrate was confirmed by electron microscopy. Briefly cell cultures were fixed for 2 h in 0.5% paraformaldehyde and 0.5% glutaraldehyde in phosphate buffer (0.1*M*, pH 7.4), washed in the same buffer and postfixed in 1% OsO4 in phosphate buffer. After dehydration in alcohols the pieces were embedded in low-viscosity epoxy resin (Spurr resin embedding kit. TAAB Laboratories Equipment Ltd, Berks, UK). Thin sections were examined in a JEOL 1200-E Il electron microscope after staining with uranyl acetate and lead citrate.

Statistical analysis

The results for each substrate were expressed as mean per field of view (×10) ±1 standard deviation (SD). Data were tested for normality and investigated for statistical significance using Student's *t*-test. Statistical significance was set at $p < 0.05$.

RESULTS

Cell adhesion

The average number of cells adhered to the ELR-IK, ELR-RGD films (each 652.8 nm thickness, Fig. 1), and glass substrates as a percentage of the polystyrene control after 4 h, as shown in figure 1, demonstrated that the average number of cells adhered to the ELR-RGD and polystyrene substrates was significantly higher ($p < 0.05$) than that attached to the other substrates after 4 h. There were no significant differences ($p > 0.05$) between the number of cells attached to the ELR-IK and glass substrates (Fig. 2).

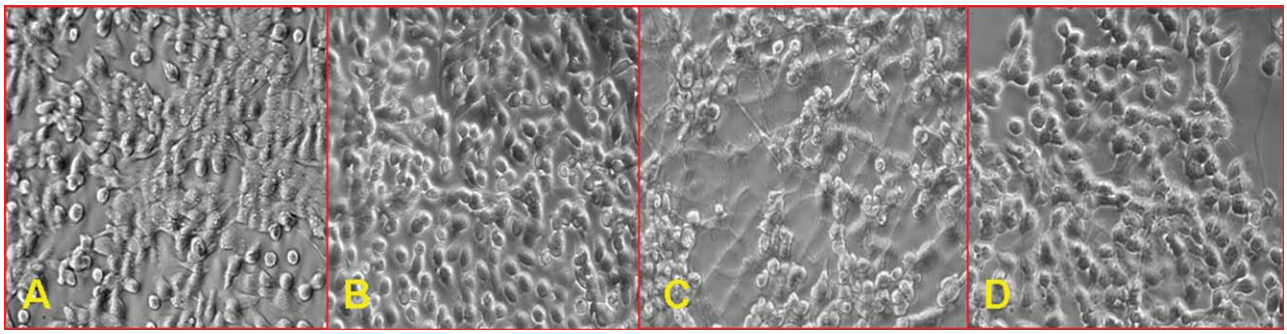

FIGURE 5. Cytotoxicity test using Trypan blue stain. ARPE19 cells growing on different substrates were stained with Trypan blue and observed under a phase-contrast microscope. The cells growing on each substrate are viable at all time points. The above pictures, taken at a field view of ×10, are representative pictures at 120 h. (A) Polystyrene; (B) glass; (C) ELR-IK; (D) ELR-RGD. [Color figure can be viewed in the online issue, which is available at wileyonlinelibrary.com.]

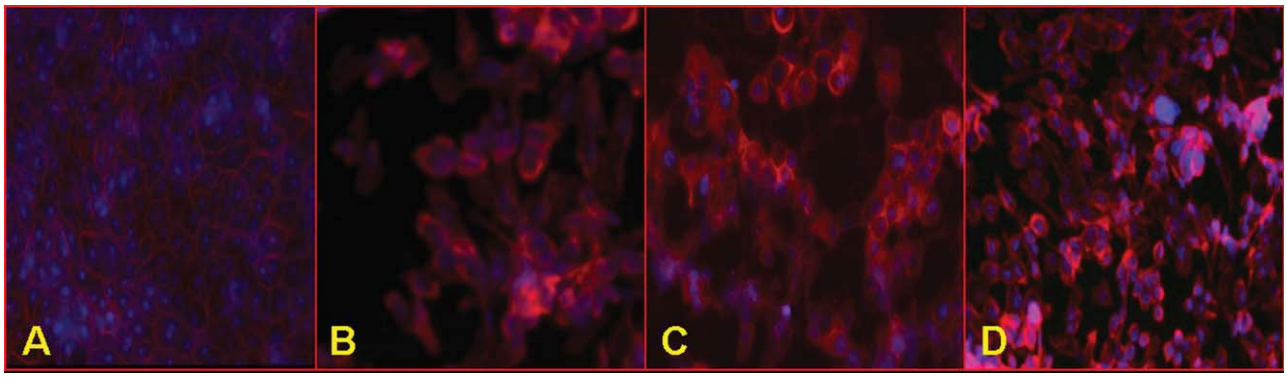

FIGURE 6. Cell morphology of ARPE19 cells on different substrates demonstrated by F-actin staining with fluorescent Rhodamin-Phalloidin stain at 120 h. A more homogenous hexagonal mosaic morphology with higher cell density is seen for polystyrene than for ELR-RGD, glass and ELR-IK. (A) Polystyrene; (B) glass; (C) ELR-IK; (D) ELR-RGD. [Color figure can be viewed in the online issue, which is available at wileyonlinelibrary.com.]

Cell proliferation

Cell proliferation was evaluated by quantifying the number of cells on the surface of all substrates at 24, 72, and 120 h, as shown in Figure 3. The histogram shows that cell growth on ELR-RGD was significantly higher ($p < 0.05$) than that found on ELR-IK at all time points (24, 72, and 120 h). However, both these films showed a significantly lower ($p < 0.05$) average number of cells on their surface than that observed on the surface of the polystyrene at all time intervals (Fig. 3). At 120 h, the cells growing on the surface of ELR-RGD, polystyrene and glass were nearly confluent, whereas the cells growing on ELR-IK needed more time to become confluent (Fig. 4), thus showing that the growth rates on ELR-RGD, polystyrene and glass are higher than on ELR-IK.

Cell viability

The Trypan blue exclusion assay was used to detect dead cells before seeding and also after growth of the cells on the different substrates. The results of this assay showed that the cells were 100% viable at the time of seeding (data not shown) and also after growing on each substrate at different time intervals (Fig. 5).

Cell morphology and RPE65 expression

Phase-contrast microscopy showed that the cells appeared to have reached confluence on the surface of all substrates, except ELR-IK, after 120 h (Fig. 4), although there was a clear difference in cell density on different substrates from the centre to the periphery. Thus, the cells growing on polystyrene surface were more closely packed and homogenous, showing a more mosaic morphology in both the central and peripheral regions, whereas the cell density and homogeneity of the mosaic pattern decreased from the centre to the periphery on the ELR-RGD, glass, and ELR-IK substrates (data not shown).

Immunofluorescence staining with Rhodamin-Phalloidin demonstrated good hexagonal circumferential actin fibers in the cells growing on all substrates (Fig. 6) while immunostaining with anti-ZO-1 antibody (Fig. 7) and electron microscopy (Fig. 8) study showed the presence of tight and gap junction confirming the epithelial morphology of the cells growing on each substrate. Under electron microscopy tight junctions (zonula occludens) were characterized by groups of union points where the plasma membranes of two adjacent cells were connected. Gap junctions (nexus) were observed as zones of membrane apposition with a dense line between the membranes (Fig. 8). A rounded cell

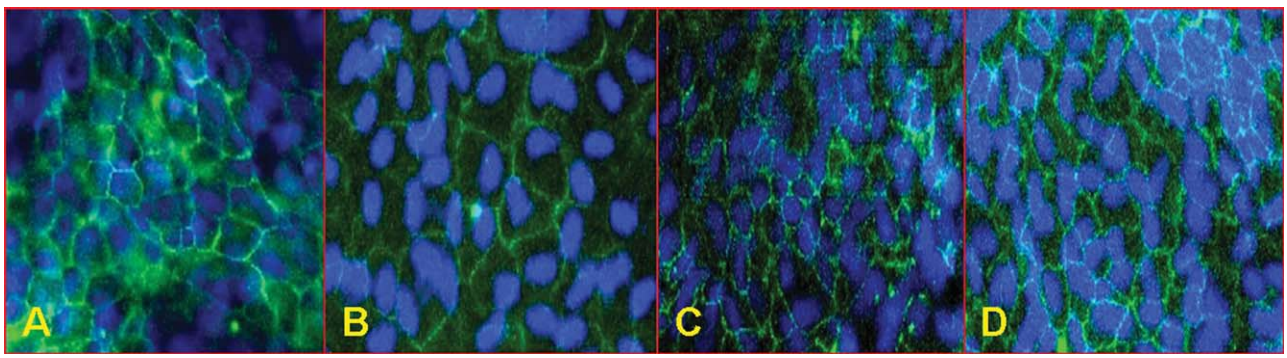

FIGURE 7. Epithelial cell morphology of ARPE19 cells on different substrates demonstrated by ZO-1 staining at 120 h. A more homogenous hexagonal mosaic epithelial morphology with higher cell density is seen for polystyrene than for ELR-RGD, glass and ELR-IK. A: Polystyrene; (B) glass; (C) ELR-IK; (D) ELR-RGD. [Color figure can be viewed in the online issue, which is available at wileyonlinelibrary.com.]

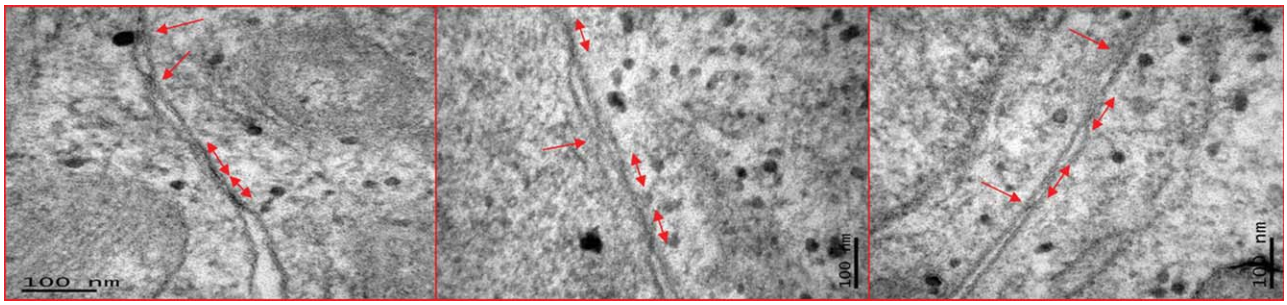

FIGURE 8. Presence of intercellular tight junctions (arrow) and gap junctions (doubleheaded arrow) among the ARPE19 cells growing on different substrates as observed by electron microscopy at 120 h. (A) Polystyrene; (B) ELR-IK; (C) ELR-RGD. [Color figure can be viewed in the online issue, which is available at wileyonlinelibrary.com.]

nucleus was observed in all cases, as detected by DAPI staining (Fig. 6 and 7).

Immunofluorescence staining with RPE65 antibody showed that the cells growing on the different substrates maintained their RPE-type characteristics and that there was no transformation into, or contamination by, other cell types (Fig. 9).

DISCUSSION

It is well known that the stimuli provided by a substrate to cells influence their behavior.[33–35] A large number of substrates, including cryoprecipitated membranes, anterior lens capsules, cadaver Bruch's membranes, Descemet's membranes, natural or synthetic biodegradable or nonbiodegradable polymers films and collagens, to name but a few, have been studied for the replacement of RPE cells.[10,36–42] Most of these, however, have proved to be either very difficult to handle or are unable to deliver and maintain appropriate signals at the level of the RPE-substrate interface. Such signals are required to maintain RPE cells in their differentiated state under *in vitro* or *in vivo* conditions. The development of an appropriate synthetic, flexible, biocompatible film with an appropriate pore size for transportation that is easy to handle during surgery and results in minimum postsurgical complications is therefore currently vital for the success of dual-layer biomimetic transplants consisting of a layer of healthy RPE cells cultured on a support membrane.[43] Such a film must also have appropriate surface characteristics that can provide the stimuli required to maintain the RPE cells in their subretinal localization. The ELR films of 652.8 nm thickness used in this study, which are composed of polymers containing repeat sequences of elastin, an extracellular elastic protein found in the vertebrate ECM, could be useful in this respect as their elastic and biocompatible characteristics are similar to those of naturally occurring ECMs and the elastic layer of BrM.[44] The recombinant nature of these polymeric films enables the insertion of peptide sequences through genetic engineering to extend their properties, including bioactive domains. These polymers have previously been used for the formation of hydrogels with different pore sizes using a salt-leaching technique.[31] ELRs biodegrade into natural amino acids by normal routes, thus allowing enough time for the transplanted cells to synthesize their own substratum and establish the correct pigment cell-neural retina architecture. Thus, the ELR films used in this study are flexible, biocompatible, biodegradable and with appropriate thickness (652.8 nm), and would appear to be highly suitable for use in RPE cell transplantation in AMD patients.

The RGD sequence is found in a number of ECM structural proteins that promote cell attachment, spreading, differentiated phenotype, and survival.[45] Indeed, in this study,

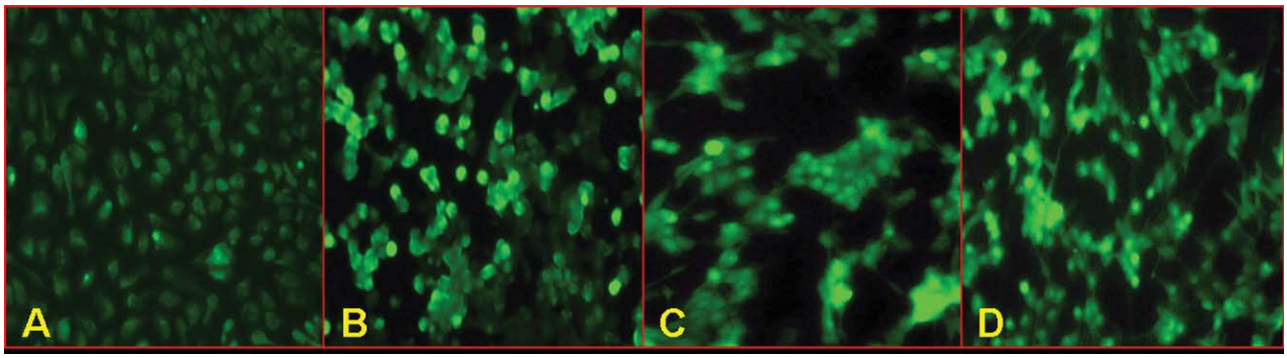

FIGURE 9. Expression of RPE65 by ARPE19 cells on different substrates. At 120 h, immunostaining with RPE65 antibody demonstrates the expression of RPE65 antigen by ARPE19 cells growing on different surfaces. (A) Polystyrene; (B) glass; (C) ELR-IK; (D) ELR-RGD. [Color figure can be viewed in the online issue, which is available at wileyonlinelibrary.com.]

interactions between RPE and RGD supported stability of RPE. Thus, the ELR must be able to maintain RPE quiescence, adherence, polarity and viability whilst also promoting proliferation after damage and migration into a wound. Therefore, inserting an RGD sequence in the bioactive domain of recombinant ELR and growing ARPE19 cells on these polymers will help to determine the suitability of this substrate for transplantation.

Despite having fewer adherences at 4 h than the polystyrene surface, ELR-RGD was nevertheless found to be a good support for the growth of ARPE19 cells. Indeed, there was a very clear difference between ELR-RGD and ELR-IK at 4, 24, 72, and 120 h. At 120 h, the difference between the number of cells attached to ELR-RGD, polystyrene and glass and those attached to ELR-IK, which did not support the growth of ARPE19 cells well, was notable. This shows that inserting bioactive sequences into ELR-IK modifies the adhesion and proliferation characteristics of the polymer and that an ELR-RGD film promotes the attachment of the cultured cells to the film. Furthermore, the total absence of dead cells, expression of RPE65 protein and presence of intracellular tight and gap junction, which means that the ARPE19 cells maintained their epithelial morphology and specificity for the whole 120-h growth period, strongly suggests that none of the ELRs used in this study are cytotoxic and that they all deliver optimal signals for promoting stability of the RPE cells including barrier formation for transportation under *in vitro* conditions. They could therefore be suitable carriers for RPE transplantation in the sub-macular region. A previous study has highlighted differences in the expression of different proteins between RPE-derived cell lines and human primary RPE cells,[46] therefore the response of human primary RPE cells to these substrates might also differ. ARPE19 cells, spontaneous immortalized RPE cells,[32] were used in this study to overcome several problems: the supply of cells, heterogeneity, the ease of culture, and the fast growth of cells as well as they have been used previously in several similar studies.[41,43] These experimental results showed that in contact with ELRs, ARPE19 cells maintained certain properties which could be useful data for further study of interaction of ELRs with primary RPE cells. In addition, as stated previously, *ex vivo* expansion of primary RPE cells leads into partial reversion of the influence of ageing but with high risk of transdifferentiation which also needs to be ruled out with cells grown on these substrates. Further studies in these respects are currently underway. Furthermore, *in vivo* studies can also lead to different responses to those observed *in vitro*. This also needs to be ruled out with further studies before an RPE-ELR transplant can be performed in a clinical setting.

In summary, genetic engineering techniques are highly suitable for the production of complex polymers with a well-defined sequence that mimic the rich complexity of the natural ECM in terms of functionality and bioactivity. Herein, a ELR containing a bioactive sequence (RGD) found in the ECM produced using such genetic engineering techniques showed good adhesion and proliferation while maintaining the phenotype of ARPE19 cells and could therefore be suitable carriers for RPE transplantation.

ACKNOWLEDGMENTS

The authors would also like to thank Alicia Rodríguez Gascón, University of País Vasco (Spain), for providing the ARPE19 cells, and Cristhian Urzua Salinas and Jesús Gómez Escudero for their help.

REFERENCES

1. Chopdar A, Chakravarthy U, Verma D. Age related macular degeneration. BMJ 2003;326:485–488.
2. Tasman W, Rovner B. Age-related macular degeneration: Treating the whole patient. Arch Ophthalmol 2004;122:648–649.
3. Friedman DS, O'Colmain BJ, Muñoz B, Tomany SC, McCarty C, de Jong PT, Nemesure B, Mitchell P, Kempen J; Eye Diseases Prevalence Research Group. Prevalence of age-related macular degeneration in the United States. Arch Ophthalmol 2004;122: 564–572.
4. Nowak JZ. Age-related macular degeneration (AMD): Pathogenesis and therapy. Pharmacol Rep 2006;58:353–363.
5. Gass JD. Drusen and disciform macular detachment and degeneration. Arch Ophthamol 1973;90:206–217.
6. da Cruz L, Chen FK, Ahmado A, Greenwood J, Coffey P. RPE transplantation and its role in retinal disease. Prog Retin Eye Res 2007;26:598–635.
7. Limb GA, Daniels JT, Cambrey AD, Secker GA, Shortt AJ, Lawrence JM, Khaw PT. Current prospects fro adult stem cell-based therapies in ocular repair and regeneration. Curr Eye Res 2006;31: 381–390.
8. Gaillard F, Sauvé Y. Cell based therapy for retina degeneration: The promise of a cure. Vision Res 2007;47:2815–2824.
9. Radtke ND, Aramant RB, Petry HM, Green PT, Pidwell DJ, Seiler MJ. Vision improvement in retinal degeneration patients by implantation of retina together with retinal pigment epithelium. Am J Ophthalmol 2008;146:172–182.
10. Binder S, Stanzel BV, Krebs I, Glittenberg C. Transplantation of the RPE in AMD. Prog Retin Eye Res 2007;26:516–554.
11. Del Priore LV, Tezel TH, Kaplan HJ. Survival of allogeneic porcine retinal pigment epithelial sheets after subretinal transplantation. Invest Ophthalmol Vis Sci 2004;45:985–992.
12. Coffey PJ, Girman S, Wang SM, Hetherington L, Keegan DJ, Adamson P, Greenwood J, Lund RD. Long-term preservation of cortically dependent visual function in RCS rats by transplantation. Nat Neurosci 2002;5:53–56.
13. van Meurs JC, ter Averst E, Hofland LJ, van Hagen PM, Mooy CM, Baarsma GS, Kuijpers RW, Boks T, Stalmans P. Autologous peripheral retinal pigment epithelium translocation in patients with subfoveal neovascular membranes. Br J Ophthalmol 2004; 88:110–113.
14. Lüke C, Alteheld N, Aisenbrey S, Lüke M, Bartz-Schmidt KU, Walter P, Kirchhof B. Electro-oculographic findings after 360 degrees retinotomy and macular translocation for subfoveal choroidal neovascularisation in age-related macular degeneration. Graefes Arch Clin Exp Ophthalmol 2003;241:710–715.
15. Wong D, Stanga P, Briggs M, Lenfestey P, Lancaster E, Li KK, Lim KS, Groenewald C. Case selection in macular relocation surgery for age related macular degeneration. Br J Ophthalmol 2004;88:186–190.
16. Binder S, Stolba U, Krebs I, Kellner L, Jahn C, Feichtinger H, Povelka M, Frohner U, Kruger A, Hilgers RD, Krugluger W. Transplantation of autologous retinal pigment epithelium in eyes with foveal neovascularization resulting from age-related macular degeneration: A pilot study. Am J Ophthalmol 2002;133:215–225.
17. Rak DJ, Hardy KM, Jaffe GJ, McKay BS. Ca++-switch induction of RPE differentiation. Exp Eye Res 2006;82:648–656.
18. Grisanti S, Guidry C. Transdifferentiation of retinal pigment epithelial cells from epithelial to mesenchymal phenotype. Invest Ophthalmol Vis Sci 1995;36:391–405.
19. Lee SC, Kwon OW, Seong GJ, Kim SH, Ahn JE, Kay ED. Epitheliomesenchymal transfifferentiation of cultured RPE cells. Ophthalmic Res 2001;33:80–86.
20. Hiscott P, Sheridan C, Magee RM, Grierson I. Matrix and the retinal pigment epithelium in proliferative retinal disease. Prog Retin Eye Res 1999;18:167–190.

21. Knoernschild T, Grasbon T, Wilsch C, Kampik A, Lütjen-Drecoll E. RPE cell transplants to non-immune-privileged sites of the eye transform into fibroblast-like cells. Curr Eye Res 2003;27:25–34.
22. Grierson I, Hiscott P, Hogg P, Robey H, Mazure A, Larkin G. Development, repair and regeneration of the retinal pigment epithelium. Eye (Lond) 1994;8:255–262.
23. Rodríguez-Cabello JC, Martín L, Alonso M, Arias FJ, Testera AM. "Recombinamers" as advanced materials for the post-oil age. Polymer 2009;50:5159–5169.
24. Girotti A, Reguera J, Arias FJ, Alonso M, Testera AM, Rodríguez-Cabello JC. Influence of the molecular weight on the inverse temperature transition of a model genetically engineered elastin-like pH-responsive polymer. Macromolecules 2004;37:3396–3400.
25. Martínez-Osorio H, Juárez-Campo M, Diebold Y, Girotti A, Alonso M, Arias FJ, Rodríguez-Cabello JC, García-Vázquez C, Calonge M Genetically engineered elastin-like polymer as a substratum to culture cells from the ocular surface. Curr Eye Res 2009;34: 48–56.
26. Di Zio K, Tirrell DA. Mechanical properties of artificial protein matrices engineered for control of cell and tissue behavior. Macromolecules 2003;36:1553–1558.
27. Lee J, Macosko CW, Urry DW. Phase transition and elasticity of protein-based hydrogels. J Biomater Sci Polym Ed 2001;12: 229–242.
28. Urry DW, Parker TM, Reid MC, Gowda DC. Biocompatibility of the bioelastic materials, poly(GVGVP) and its -irradiation cross-linked matrix: Summary of generic biological test results. J Bioact Compat Polymers 1991;6:263–282.
29. Berg MC, Yang SY, Hammond PT, Rubner MF. Controlling mammalian cell interactions on patterned polyelectrolyte multilayer surfaces. Langmuir 2004;20:1362–1368.
30. Ruoslahti E. RGD and other recognition sequences for integrins. Annu Rev Cell Dev Biol 1996;12:697–715.
31. Martín L, Alonso M, Girotti A, Arias FJ, Rodríguez Cabello JC. Synthesis and characterization of macroporous thermo sensitive hydrogels from recombinant elastin-like polymers. Biomacromolecules 2009;10:3015–3022.
32. Dunn KC, Aotaki-Keen AE, Putkey FR, Hjelmeland LM. ARPE-19, a human retinal pigment epithelial cell line with differentiated properties. Exp Eye Res 1996;62:155–169.
33. Berg MC, Yang SY, Hammond PT, Rubner MF. Controlling mammalian cell interactions on patterned polyelectrolyte multilayer surfaces. Langmuir 2004;20:1362–1368.
34. Zarbin MA. Analysis of retinal pigment epithelium integrin expression and adhesion to aged submacular human Bruch's membrane. Trans Am Ophthalmol Soc 2003;101:499–520.
35. Gullapalli VK, Sugino IK, Zarbin MA. Culture-induced increase in alpha integrin subunit expression in retinal pigment epithelium is important for improved resurfacing of aged human Bruch's membrane. Exp Eye Res 2008;86:189–200.
36. Sheridan C, Williams R, Grierson I. Basement membranes and artificial substrates in cell transplantation. Graefes Arch Clin Exp Ophthalmol 2004;242:68–75.
37. Sheridan C, Krishna Y, Williams R, Mason S, Wong D, Heimann H, Kent D, Grierson I. Transplantation in the treatment of age-related macular degeneration: Past, present and future directions. Expert Rev Ophthalmol 2007;2:1–14.
38. Ma Z, Han L, Wang C, Dou H, Hu Y, Feng X, Xu Y, Wang Z, Yin Z, Liu Y. Autologous transplantation of retinal pigment epithelium-Bruch's membrane complex for hemorrhagic age-related macular degeneration. Invest Ophthalmol Vis Sci 2009;50:2975–2981.
39. Maaijwee K, Van Den Biesen PR, Missotten T, Van Meurs JC. Angiographic evidence for revascularization of an rpe-choroid graft in patients with age-related macular degeneration. Retina. 2008;28:498–503.
40. Neeley WL, Redenti S, Klassen H, Tao S, Desai T, Young MJ, Langer R. A microfabricated scaffold for retinal progenitor cell grafting. Biomaterials 2008;29:418–426.
41. Lu JT, Lee CJ, Bent SF, Fishman HA, Sabelman EE. Thin collagen film scaffolds for retinal epithelial cell culture. Biomaterials 2007; 28:1486–1494.
42. Thumann G, Hueber A, Dinslage S, Schaefer F, Yasukawa T, Kirchhof B, Yafai Y, Eichler W, Bringmann A, Wiedemann P. Characteristics of iris and retinal pigment epithelial cells cultured on collagen type I membranes. Curr Eye Res 2006;31:241–249.
43. Lee CJ, Fishman HA, Bent SF. Spatial cues for the enhancement of retinal pigment epithelial cell function in potential transplants. Biomaterials 2007;28:2192–2201.
44. Booij JC, Baas DC, Beisekeeva J, Gorgels TG, Bergen AA. The dynamic nature of Bruch's membrane. Prog Retin Eye Res 2010;29: 1–18.
45. Ruoslahti E. RGD and other recognition sequences for integrins. Annu Rev Cell Dev Biol 1996;12:697–715.
46. Alge CS, Hauck SM, Priglinger SG, Kampik A, Ueffing M. Differential protein profiling of primary versus immortalized human RPE cells identifies expression patterns associated with cytoskeletal remodeling and cell survival. J Proteome Res 2006;5:862–878.